Appl. Phys. A 33, 63–76 (1984)

Applied Physics A Solids and Surfaces

Selectively Doped n-$Al_xGa_{1-x}As$/GaAs Heterostructures with High-Mobility Two-Dimensional Electron Gas for Field Effect Transistors

Part I. Effect of Parallel Conductance

E. F. Schubert and K. Ploog

Max-Planck-Institut für Festkörperforschung, D-7000 Stuttgart 80, Fed. Rep. Germany

H. Dämbkes and K. Heime

Universität Duisburg, Fachgebiet Halbleitertechnik/Halbleitertechnologie, D-4100 Duisburg 1, Fed. Rep. Germany

Received 15 July 1983/Accepted 29 August 1983

Abstract. In selectively doped n-$Al_xGa_{1-x}As$/GaAs heterostructures with high-mobility two-dimensional electron gas (2 DEG) at the heterointerface a second conductive channel exists, if the $Al_xGa_{1-x}As$ layer is not totally depleted from free carries. The occurrence of parallel conductance has a deleterious effect on the performance of high-electron mobility transistors (HEMTs) fabricated from this material. Although in principle computable, parallel conductance depends on a large number of design parameters to be chosen for the heterostructure, which are additionally affected by the presence of deep electron traps in n-$Al_xGa_{1-x}As$ of composition $0.25 < x < 0.35$. Capacitance-voltage, Hall effect, and transverse magnetoresistance measurements in the temperature range 4–300 K were used to detect the undesired parallel conductance and to demonstrate its effect on the result of these evaluation techniques. In addition, the significant influence of parallel conductance on the dc properties of HEMTs fabricated from selectively doped n-$Al_xGa_{1-x}As$/GaAs heterostructures is shown.

PACS: 68.55.+b, 72.00.Fr, 73.40.Lq, 85.30.De

In selectivity doped n-$Al_xGa_{1-x}As$/GaAs heterostructures only the wider gap semiconductor $Al_xGa_{1-x}As$ is intentionally doped with Si donors while the smaller gap material is left nominally undoped. Due to the conduction band discontinuity at the heterointerface, ΔE_c, electrons from the donors in the $Al_xGa_{1-x}As$ layer are transferred to the adjacent undoped GaAs layer, where they form a quasi-two-dimensional electron gas (2 DEG). As a result, the electrons which occupy quantum well states up to the Fermi level E_F are now spatially separated from their parent ionized impurities. The basic idea, first verified by Dingle et al. [1] in their concept of modulation doping, is that in this configuration the free-electrons can propagate within the GaAs layer with strongly reduced probability of being scattered by donor impurities. Mobility enhancement is greatest in heterostructures where thin undoped spacer layers are inserted [2], i.e. a $Al_xGa_{1-x}As$ region of 5–10 nm near the interface is left undoped. Very high-mobilities are obtained particularly at low-temperatures where reduction of Coulomb scattering is most pronounced (see also Fig. 8 for illustration).

The introduction of modulation or selectively doping greatly extended the underlying physics of $Al_xGa_{1-x}As$/GaAs heterostructures and quantum well structures to totally new fundamental problems, including quantized Hall effect [3], near-zero-

resistance state [4], electron localization in a 2 DEG in strong magnetic fields [5, 6] etc. Furthermore, a new device concept called high-electron mobility transistor (HEMT) [7] or two-dimensional electron gas field effect transistor (TEG FET) [8] has been developed from these structures for high-speed logic application. In these devices, a significantly higher transconductance was obtained at 77 K as compared to 300 K, due to the stronlgy enhanced low-temperature mobility. In addition, lower noise-figures than in comparable GaAs MESFETs have been measured [9, 10].

As expected, the design parameters of the selectivity doped n-$Al_xGa_{1-x}As$/GaAs heterostructures, i.e. doping concentration, alloy composition, layer thicknesses etc., are found to be of crucial importance for the performance and device characteristics of HEMTs. In particular, if the doped $Al_xGa_{1-x}As$ region is not totally depleted from free carriers, a conductance parallel to the 2 DEG can occur which has a deleterious effect on the device performance. In this paper we present the results of a detailed investigation on the origin and detection of parallel conductance in selectively doped n-$Al_xGa_{1-x}As$/GaAs heterostructures. For experimental evaluation, we used capacitance-voltage (C-V), Hall effect and conductivity, and magnetotransport (Shubnikov-de Haas) measurements in the temperature range 4–300 K. Finally, we discuss the influence of parallel conductance on the properties of high-electron mobility transistors.

1. Experimental

The selectively doped n-$Al_xGa_{1-x}As$/GaAs heterostructures were grown by molecular beam epitaxy (MBE) in a system of the horizontal evaporation type which was equipped with a sample transfer device, a two-inch diameter rotating substrate holder, and an extended LN_2 cryopanel encircling the whole growth area. The layered structure, schematically shown in Fig. 1, was deposited simultaneously onto (100) oriented semi-insulating and on heavily Si-doped n^+-GaAs substrate wafers soldered side by side with liquid In on the Mo mounting and transfer plate. GaAs was grown at a substrate temperature ranging from 580°–600 °C, while for $Al_xGa_{1-x}As$ a growth temperature of 650°–660 °C had to be used to improve the material quality [11, 12]. The temperature of the Ga effusion cell was kept constant resulting in a growth rate of 1.0 µm/h for GaAs. The temperatures of the Al and Si effusion cells were systematically varied to obtain the desired alloy compositions of $x=0.25$ to 0.35 and donor concentrations of $N_D=1.0$ to $2.5\times10^{18}\,cm^{-3}$ in the various samples. The arsenic flux was adjusted to yield a slightly As-stabilized (2×4) surface reconstruction.

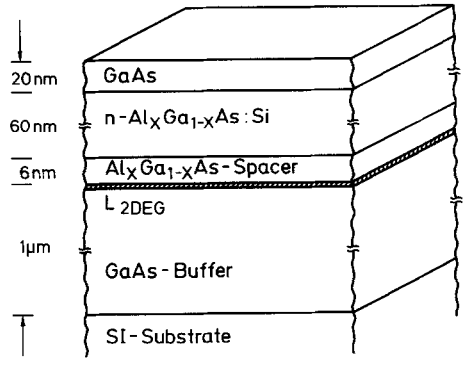

Fig. 1. Schematic arrangement of layer sequence in selectively doped n-$Al_xGa_{1-x}As$/GaAs heterostructures

The selectively doped heterostructures used for the present investigation consisted of four layers as depicted in Fig. 1. The 1 µm thick undoped GaAs buffer layer was p-type in the high $10^{14}\,cm^{-3}$ range due to residual carbon doping. A 5–10 nm thick undoped $Al_xGa_{1-x}As$ spacer increased the spatial separation of the 2 DEG from the parent ionized donor impurities. The Si-doped n-$Al_xGa_{1-x}As$ layer ($N_D=1.0-2.5\times10^{18}\,cm^{-3}$) had a thickness of 50–60 nm. In the various samples an alloy composition of $x=0.25$ and $x=0.30$ was chosen to provide a sufficient barrier height at the heterointerface and to keep the overall electron trap concentration, which increases with x, as low as possible [13, 14]. The alloy composition of the samples was controlled by photoluminescence measurements using the method proposed by Dingle et al. [15] and occasionally also by Raman scattering [16]. On top of the n-$Al_xGa_{1-x}As$:Si layer a 10–20 nm thick GaAs cladding layer was deposited to protect the reactive $Al_xGa_{1-x}As$ surface and to facilitate metallization for rectifying (Schottky) contacts. The continuous rotation of the substrate during growth (3–6 rpm) had to be synchronized to growth rate and layer thickness for a good uniformity of doping concentration, alloy composition and layer thickness also over large area (2 inch) substrates.

The C-V profiling measurements were performed on reverse-biased 1 mm diameter Schottky diodes fabricated by evaporating 200 nm Al onto the as-grown surface of the GaAs cladding layer of the sample kept at $T<20\,°C$ in a separate vacuum chamber. In some cases, we used the non-destructive Hg-probe technique for the C-V measurements. There were no marked differences in the profiling results obtained from the two metals for the Schottky diodes. The observed diode characteristics were as follows: diode n-value $n<1.20\pm0.10$, saturation currents $I_s=1.5\times10^{-8}$ A/cm^2, and barrier height $\Phi_B=0.95\pm0.05$ V. The C-V measurements were carried out at room temperature with a frequency of $10^6\,s^{-1}$ using a fully automated measurement and data handling routine [17].

Hall effect and conductivity measurements in the temperature range 4.2–300 K as well as magneto-transport measurements at 4.2 K were performed on photolithographically defined Hall-bars, each having six symmetrically placed side arms in addition to drain and source contact area (Hall measurements on rectangular shaped samples using the van der Pauw technique showed only minor differences within the experimental error). Ohmic contacts were formed either by placing small Sn balls or by evaporating photolithographically defined planar Sn–Au contacts (20 nm and 200 nm, respectively) on the Hall device, followed by 4 min alloying at 380 °C in flowing N_2/H_2 (80 : 20 %) gas. The relatively low annealing temperature and short annealing time were chosen to avoid a lateral diffusion of Sn at the heterointerface that could lead to a degradation of the 2 DEG. The temperature dependence of the Hall effect was measured in an automated system controlled by a programmable desk-top calculator [17]. The sample was mounted on a Cu block in a variable temperature continuous flow cryostat. The flow rate of liquid He, the setting of the temperature controller, and the reversion of the polarity of the magnetic field were all set and monitored by the calculator. For illumination of the sample we used a GaAs LED to avoid band-to-band excitation in the $Al_xGa_{1-x}As$ layer. The standard magnetic induction for these experiments was 0.5 T, and for some measurements the magnetic induction was varied stepwise from 0.05 T to 0.5 T.

Finally, we performed measurements of the transverse magnetoresistance (Shubnikov-de Haas effect) at low-temperatures to probe directly the 2 DEG at the heterointerface. The bar-shaped sample of 3.5 mm length × 0.4 mm width (a large length-to-width ratio is required in order to reduce the influence of the electrodes) was placed in a liquid He bath cryostat together with a superconducting solenoid. The magnetic induction, calibrated to better than 3 %, was applied perpendicular to the plane of the 2 DEG and swept from zero up to 7.5 T. The data were obtained by measuring the voltage between appropriate side arms (potential probes) of the sample with a high-input-impedance nano-voltmeter when a direct current of 1 μA was supplied to drain and source. A GaAs LED was used for illumination of the sample.

2. Real-Space Conduction Band Diagram and Calculation of 2D Sheet Carrier Concentration

In Fig. 2 we show schematically the real-space conduction band diagram of a selectively doped n-$Al_xGa_{1-x}As$/GaAs heterostructure where the 2D accumulation channel is located below the Si-doped n-$Al_xGa_{1-x}As$ layer. In the ideal case, the $Al_xGa_{1-x}As$ is totally depleted and all mobile electrons are confined to the 2 DEG region. The general trend in the correlation between 2D sheet carrier concentration, $n_{2\,DEG}$, and given doping concentration of the $Al_xGa_{1-x}As$, N_D, is that $n_{2\,DEG}$ decreases with increasing spacer width, W_S, and increases with enhanced Al mole fraction.

For a more accurate calculation of the 2D sheet carrier concentration vs. design parameters of the heterostructure we have to introduce the following relations between the various widths, W, and potential drops, V, of the constituent layers derived from simple electrostatic considerations (see also Fig. 2 for illustration). The width of the (top) GaAs cladding layer, W_c, is related to the corresponding potential, V_c, by

$$V_C = 2V_{bi}^S \frac{W_C}{W_{DS}}, \tag{1}$$

where V_{bi}^S is the built-in voltage near the surface. The depletion width near the surface, W_{DS}, is given by

$$W_{DS} = \left(\frac{2\varepsilon_1}{qN_D} V_{bi}^S\right)^{1/2} \tag{2}$$

with

$$V_{bi}^S = \Phi_B - V_C + \frac{\Delta E_C}{q} - \xi, \tag{3}$$

where ε_1 is the permittivity of $Al_xGa_{1-x}As$, q is the elementary charge, Φ_B is the surface barrier height for GaAs (= 0.7 V [18]), $\Delta E_C = 0.85 \Delta E_g$ [19], and ξ is the distance between the conduction band, E_C, and the Fermi level in the not depleted $Al_xGa_{1-x}As$ region. For the interface depletion width, W_D, we have the relation

$$W_D = n_{2\,DEG}/N_D \tag{4}$$

with

$$V_{bi} = \frac{q n_{2\,DEG}^2}{2\varepsilon_1 N_D} \tag{5}$$

and the spacer width, W_S, is related by

$$V_S = \frac{q n_{2\,DEG}}{\varepsilon_1} W_S \tag{6}$$

to the potential V_S. If we assume that $\xi = 0$, which is reasonable for the doping range we used ($N_D = 1$ to 2×10^{18} cm^{-3}), and use (1)–(3), the depletion width, W_{DS}, can be expressed by

$$W_{DS} = \left[W_c^2 + \frac{2\varepsilon_1}{q \cdot N_D}\left(\Phi_B + \frac{\Delta E_c}{q}\right)\right]^{1/2} - W_c. \tag{7}$$

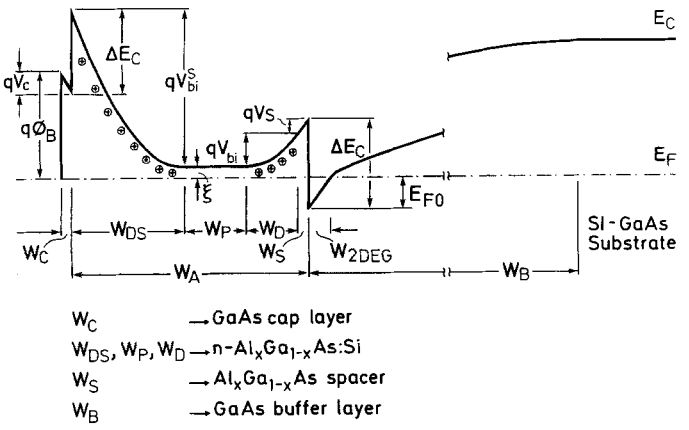

Fig. 2. Conduction band diagram of selectively doped n-$Al_xGa_{1-x}As$/GaAs heterostructures with 2DEG at the heterointerface (not drawn to scale)

In this first approximation the contribution of deep traps in the $Al_xGa_{1-x}As$ layer has been neglected in (4).

Calculation of the sheet carrier concentration in the highly degenerate 2DEG implies that Fermi-Dirac statistics have to be used instead of the simpler Maxwell-Boltzmann statistics. Two analytic approximations are in general employed for the Fermi-Dirac integral; the Ehrenberg approximation [20] and the Joyce-Dixon (JD) approximation [21]. We use the JD approximation for our present calculations because this approach is valid up to a higher degeneracy. Further, we assume that the GaAs buffer is compensated, i.e. i-GaAs, according to our previous investigations, and we neglect any quantum size effect. Using the JD approximation the difference of the Fermi energy and the energy of the conduction band in the i-GaAs, $E_F - E_C$, (see Fig. 2) can be expressed by:

$$\frac{E_F - E_C}{kT} = \ln\frac{n}{N_C} + \sum_m A_m \left(\frac{n}{N_C}\right)^m \quad \text{for} \quad 1 \leqq m \leqq 4, \tag{8}$$

where $n = n(z)$ is the free-electron concentration depending on the distance from the heterointerface, z, and N_C is the effective density of states at the bottom of the conduction band. The coefficients A_m are given in [21]. We proceed to differentiate (8) with respect to z and multiply the derivative with Poisson's equation

$$\frac{dE}{dz} = qn/\varepsilon_2, \tag{9}$$

where ε_2 is the permittivity of GaAs, and we finally integrate the resulting expression with the boundary condition $E = 0$ for $n(z \to \infty) \simeq 0$ and obtain the electric field E at the heterointerface, i.e. at $z = 0$

$$\frac{\varepsilon_2 E^2}{2kT} = N_C \sum_m B_m \left(\frac{n}{N_c}\right)^m. \tag{10}$$

The coefficients B_m are given by

$$B_m = 1 \quad \text{for} \quad m = 1$$
$$\text{and} \tag{11}$$
$$B_m = \frac{m-1}{m} A_{m-1} \quad \text{for} \quad 2 \leqq m \leqq 5.$$

If we eliminate the electric field in (10) using Gauß's law

$$n_{2\,\mathrm{DEG}} = -\varepsilon_2 E/q \tag{12}$$

we obtain, taking (8) into account, a relationship between $n_{2\,\mathrm{DEG}}$ and the Fermi level at the interface, $E_{F0} = E_F - E_C(z=0)$, which is displayed in Fig. 3.

Inspection of Fig. 2 reveals that

$$\Delta E_C = E_{F0} + \xi + qV_{bi} + qV_S. \tag{13}$$

Using (5) and (6) we obtain

$$\Delta E_C = E_{F0} + \xi + \frac{q^2 n_{2\,\mathrm{DEG}}}{2\varepsilon_1 N_D} + \frac{q^2 n_{2\,\mathrm{DEG}}}{\varepsilon_1} W_S. \tag{14}$$

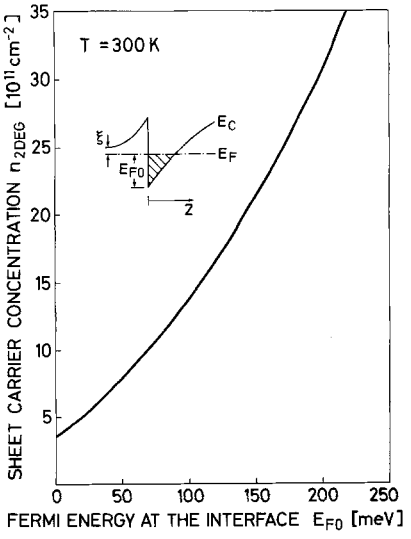

Fig. 3. Sheet carrier concentration $n_{2\,\mathrm{DEG}}$ vs. Fermi level E_{F0} at the interface obtained from Fermi-Dirac statistics using the Joyce-Dixon approximation

The donor concentration is given by the relation

$$N_D = N_C \exp -\frac{\xi}{kT}\left(1 + g \exp \frac{E_C - E_D - \xi}{kT}\right), \quad (15)$$

where $g=2$ is the ground state degeneracy of the donor level and $(E_C - E_D)$ is taken to be 45 meV, as will be explained in Sect. 3.2. For each concentration $n_{2\,DEG}$, which in turn determines the value of E_{F0} (Fig. 3), we obtain the corresponding value of N_D via (14) and (15) performing the numerical calculation by means of Newton's method. In Fig. 4 we show the results of the calculations for various spacer widths and for the Al mole fractions of $x=0.25$ and $x=0.35$.

In addition, we can calculate the required thickness of the Si-doped region of the $Al_xGa_{1-x}As$ layer if W_C, W_S, N_D, and x are known. Using (4) and (7) and the plot of Fig. 4 we present two examples:

(i) $W_C = 10$ nm, $W_S = 5$ nm, $x=0.35$, $N_D = 1 \times 10^{18}$ cm^{-3}: Thickness of Si-doped n-$Al_xGa_{1-x}As$: 46 nm.

(ii) W_C, W_S, N_D same as above, $x=0.25$: Thickness of Si-doped n-$Al_xGa_{1-x}As$: 41 nm.

The approximations used for the present calculation provide reasonable agreement with the experiments. More precise calculations of $n_{2\,DEG}$ require complex self-consistent methods which have been introduced by Ando et al. [22].

Both depletion regions of the heterostructure, at the surface and 2DEG interface, can be considered to be totally depleted from free-carriers. In addition, the transitions from the neutral region (W_p) to the two space charge regions (W_{DS} and W_D) are abrupt, since the Debye length (2–3 nm at the used doping level) is much shorter than the depletion widths. In Fig. 2 we have depicted the situation that the two depletion regions do not touch each other. Between both regions there is still an undepleted region of width W_p, where free electrons contribute to the overall conductivity of the heterostructure. When the total thickness of the $Al_xGa_{1-x}As$ layer exceeds the sum $(W_{DS} + W_D + W_S)$, parallel conductivity occurs.

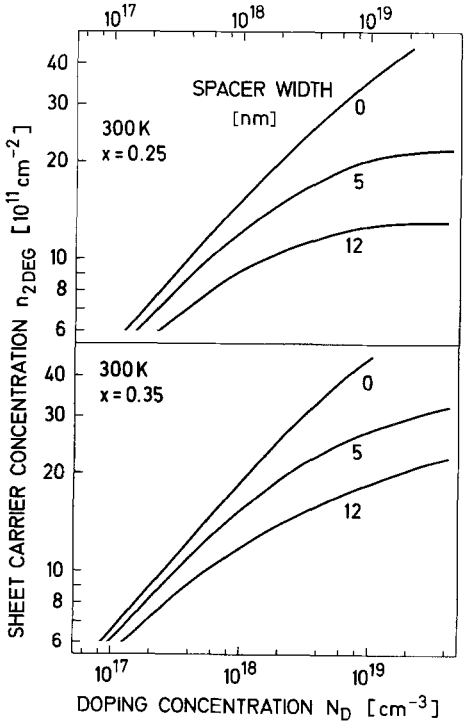

Fig. 4. Calculated dependence of sheet carrier concentration $n_{2\,DEG}$ on Al mole fraction, spacer width, and Si doping concentration in selectively doped n-$Al_xGa_{1-x}As$/GaAs heterostructures

Equations (4) and (7) demonstrate that the occurrence of parallel conductance in selectively doped n-$Al_xGa_{1-x}As$/GaAs heterostructures depends on a number of design parameters: thickness of undopted $Al_xGa_{1-x}As$ spacer layer, thickness of doped $Al_xGa_{1-x}As$ region, thickness of GaAs cladding layer, doping concentration, and Al-mole fraction. The situation becomes even more complicated if deep electron traps are present in the $Al_xGa_{1-x}As$ layer. We have recently shown [14, 23] that several deep traps are present in the $Al_xGa_{1-x}As$ layer and that their concentration depends on the Al-mole fraction and also on the growth temperature. In this case, the "effective" doping concentration $N^+_{D\,eff}$ is given by

$$N^+_{D\,eff} = N^+_D - N^-_T, \quad (16)$$

where N^-_T is the concentration of ionized deep traps. The effective doping concentration from the doped $Al_xGa_{1-x}As$ region can thus be reduced significantly as N^-_T increases. Furthermore, we can change the charge of deep traps by illuminating the sample with light of energy below the band gap [24]. In this process, the electrons are photoexcited persistently from the deep traps to the conduction band of the ternary alloy and thus enhance the effective doping concentration $N^+_{D\,eff}$. The dependence of parallel conductance on this large number of sensitive design parameters implies that the judicious change of one parameter (e.g. doping concentration) requires the adjustment of one or two other parameters to avoid this undesired effect.

3. Results and Discussion

3.1. Capacitance-Voltage Depth Profiling Measurements

Capacitance-voltage profiling using the differential capacitance is a well-established technique to determine the spatial distribution of the free electrons also in a non-uniformly doped semiconductor [24]. This information is then used to determine the doping (donor) distribution. However, the method does not

yield the correct doping profile in space charge regions. Therefore, the *apparent* doping profile obtained from the selectively doped n-$Al_xGa_{1-x}As$/GaAs four-layer heterostructure, where the Schottky barrier is adjacent and parallel to the heterojunction, does not represent the true local donor concentration profile. In the following we estimate the doping profile that can be expected from a selectively doped n-$Al_xGa_{1-x}As$/GaAs heterostructure without any parallel conductance and compare it with our experimental results. As a first approximation, we assume the presence of homogeneous material having the dielectric constant of GaAs.

When we apply a negative bias and a superimposed ac-voltage to the Schottky contact, the carrier concentration $n_{2\,\mathrm{DEG}}$ can be modulated according to

$$q \cdot \Delta n_{2\,\mathrm{DEG}} = C \cdot \Delta V. \tag{17}$$

Here C is the capacitance per unit area and ΔV is the ac-component of the applied voltage. The capacitance C is given by the spatial separation of the 2 DEG and the adjacent parallel Schottky contact. As this separation remains nearly unchanged with bias variation, the observed capacitance is a constant as long as $n_{2\,\mathrm{DEG}}$ is modulated. The apparent doping concentration N_D^* follows then from the proportionality

$$N_D^* \sim \left(\frac{d(1/C^2)}{dV}\right)^{-1}. \tag{18}$$

From this relation, the apparent doping concentration derived from C-V data should therefore approach infinity. In practice, very high values are actually reached.

In Fig. 5 we show the apparent doping profile obtained from a sample where the constituent Si-doped $Al_xGa_{1-x}As$ layer is not completely depleted. The doping concentration in this layer approaches $10^{18}\,\mathrm{cm}^{-3}$ according to this measurement. When we start to deplete the 2 DEG by increasing the reverse bias, the apparent doping concentration increases drastically to a value of $10^{19}\,\mathrm{cm}^{-3}$. This steep increase can only be caused by the 2 DEG, as such a high level cannot be achieved in homogeneously Si-doped GaAs [26]. In this particular sample the depth profiling measurement was limited by the breakdown voltage of the Schottky diode. The observed apparent doping profile, however, clearly demonstrates that the 2 DEG is strongly bypassed by not depleted free electrons in the $Al_xGa_{1-x}As$ layer.

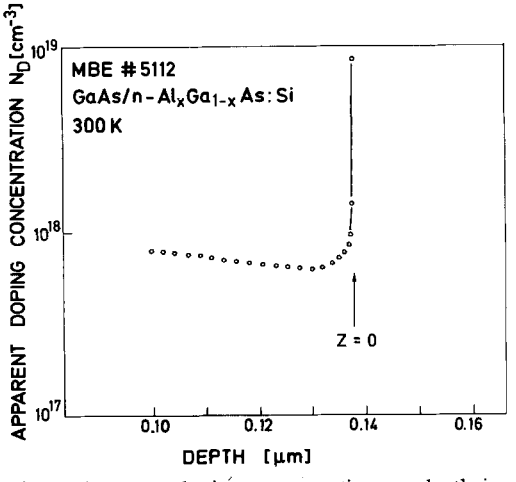

Fig. 5. Apparent doping concentration vs. depth in a selectively doped n-$Al_xGa_{1-x}As$/GaAs heterostructure with parallel conductance measured by C-V profiling

Inspection of Fig. 5 further reveals that the measured profile places the 2 DEG at a larger depth than expected from the geometry of the heterostructure. The difference is approximately 50% which we explain as follows. Since we assumed homogeneous material in our approximation for data evaluation, we have actually to discriminate between the apparent depth W_A and the real depth W_R of the 2 DEG using the relations

$$W_R = W_I + W_C + W + \tfrac{1}{2} W_{2\,\mathrm{DEG}}, \tag{19}$$

$$W_A = \frac{\varepsilon_2}{\varepsilon_I} W_I + W_C + \frac{\varepsilon_2}{\varepsilon_1} W + \tfrac{1}{2} W_{2\,\mathrm{DEG}}, \tag{20}$$

where W is the thickness of the $Al_xGa_{1-x}As$ layer and W_I and ε_I are the unknown width and the permittivity of an interfacial layer between the Schottky contact and the semiconductor. The dielectric constants of both the $Al_xGa_{1-x}As$ and of the interfacial layer are smaller than that of GaAs. Consequently, in our evaluation procedure the apparent (observed) depth obtained from C-V profiling is larger than the actual depth.

In selectively doped n-$Al_xGa_{1-x}As$/GaAs heterostructure with no detectable parallel conductance, the depletion of the 2 DEG during C-V profiling begins already at zero bias voltage. In Fig. 6 this situation is illustrated in detail. At the apparent depth of the 2 DEG which is now the beginning of carrier detection, a declining concentration peak is observed which smoothly decreases with depth. It is well established that the spatial resolution of the C-V profiling technique for abrupt change in carrier concentration is limited by majority carrier diffusion [24]. Therefore, the expected sharp transition from the 2 DEG into the GaAs buffer layer underneath is smoothed out by the increasing Debye length ($\lambda_{\mathrm{Debye}} \sim 1/\sqrt{n}$ [27]). Since this GaAs buffer layer below the electron accumulation channel is already totally depleted in the ideal case, the Debye length in this region becomes even larger.

Inspection of the two carrier profiles shown in Figs. 5 and 6 clearly indicates that a rough distinction between selectively doped n-$Al_xGa_{1-x}As$/GaAs heterostruc-

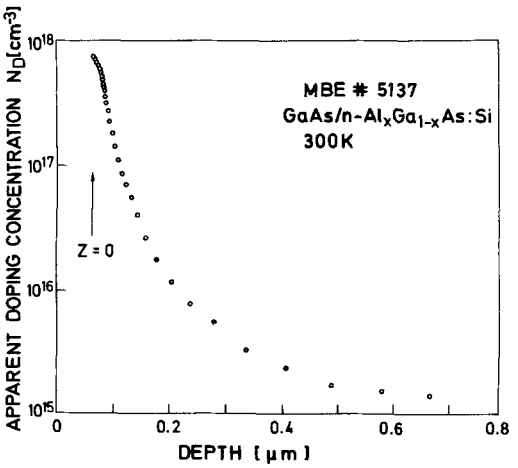

Fig. 6. Apparent doping concentration vs. depth in a selectively doped n-$Al_xGa_{1-x}As$/GaAs heterostructure with *no* parallel conductance obtained by C-V profiling

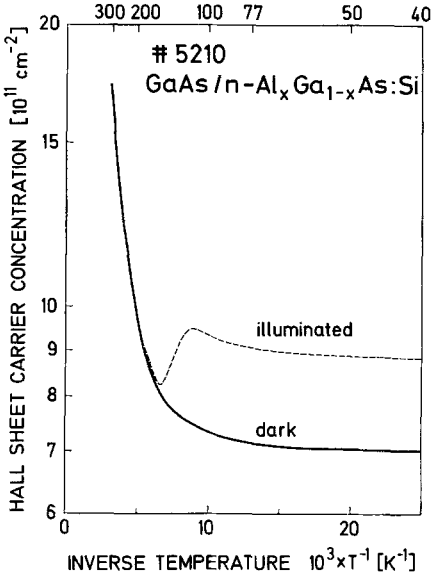

Fig. 7. Hall sheet carrier concentration vs. inverse temperature obtained from a representative selectively doped n-$Al_xGa_{1-x}As$/GaAs heterostructure in the dark and after illumination with light of energy below the bandgap of $Al_xGa_{1-x}As$

tures having an undesired marked parallel conductance and those having only the ideal 2DEG can already be obtained from fairly simple C-V profiling measurements. The technique works also at low-temperatures, but it is not applicable to structures with only a slight parallel conductance (in the $Al_xGa_{1-x}As$) and for detection of any paralell conductance within the GaAs buffer-layer/substrate region.

3.2. *Hall Effect and Conductivity Measurements*

The data derived from Hall effect measurements on selectively doped n-$Al_xGa_{1-x}As$/GaAs heterostructures in the temperature range 4–300 K are presented in Figs. 7 and 8. For a representative sample (No. 5210) we obtained a room-temperature mobility of 5000 cm^2/Vs with a sheet carrier concentration of 1.6×10^{12} cm^{-2}. At 77 K the carrier density dropped to 7.1×10^{11} cm^{-2}, while the electron mobility increased drastically to a value of 86,000 cm^2/Vs. With respect to application of this material to high-speed devices, it is important that these high-mobilities are achievable with sufficiently high-carrier densities at the economically feasible temperature of 77 K (a density of 7×10^{11} cm^{-2} in the 2DEG corresponds to an interparticle distance equivalent to a three-dimensional concentration of $\sim1\times10^{18}$ cm^{-3}).

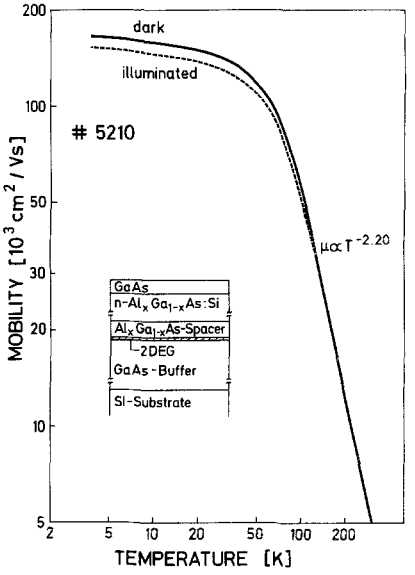

Fig. 8. Hall mobility vs. temperature obtained from a representative selectively doped n-$Al_xGa_{1-x}As$/GaAs heterostructure in the dark and after illumination with light of energy below the bandgap of $Al_xGa_{1-x}As$

More detailed information on the sharp decrease of carrier density with inverse temperature is obtained from the plot of Fig. 7. In the dark we observed an exponential decrease of the carrier density below room-temperature. The activation energy for this freeze-out of free carriers into the dominant deep level of the $Al_xGa_{1-x}As$: Si layer can be calculated as a first approximation from the relation

$$n\sim\exp-\left(\frac{E_C-E_D}{2kT}\right) \tag{21}$$

and yields approximately 45 meV (the actual value depends on the doping concentration of the ternary alloy [14]). At temperatures below 100 K the measured carrier density saturates at a level of 7.1×10^{11} cm^{-2}. This constant value is that of the 2DEG at the

interface since it agrees well with the value determined by magneto-resistance measurements at 4.2 K (see Sect. 3.3).

After exposure of the sample to light having an energy below the gap of $Al_{0.3}Ga_{0.7}As$, at low-temperature, the carrier density is found to increase and saturate at a value of $9 \times 10^{11}\,cm^{-2}$. This density increase persists in the dark after illumination ended. Although the original 300 K carrier density is not reached after light exposure in this specific selectively doped sample, the observed behaviour clearly corresponds to the low-temperature persistent photoconductivity effect reported earlier, which we have recently analyzed in detail [28]. According to this analysis the persistent photoconductivity effect in n-$Al_{0.3}Ga_{0.7}As$:Si bulk originates from deep donor-type (D,X) centers which are homogeneously distributed throughout the material and which can be optically activated. Since tunneling rates across the interface barrier of the present heterostructure are sufficiently high, the photo-excited electrons transfer partially to the GaAs underneath adding to the electrons of the 2 DEG. Therefore, this effect can be employed to vary the density of the 2 DEG of a given sample continuously over a considerable concentration range. It is important, however, that this illumination of selectively doped n-$Al_xGa_{1-x}As$/GaAs heterostructures can also lead to the undesired parallel conductance, as described in Sect. 3.3.

Figure 8 shows the mobility as a function of temperature obtained from a representative sample (No. 5210) by Hall effect measurements both in the dark and after illumination. This μ vs. T curve is characteristic for selectively doped n-$Al_xGa_{1-x}As$/GaAs heterostructures in that its mobility keeps increasing down to the lowest temperature. While at room-temperature polar phonon scattering of the carriers similar to the process in bulk GaAs is dominant, the strong reduction of mobility found in the low-temperature regime of bulk material due to ionized impurity scattering is lacking. At 77 K the mobility reaches $86{,}000\,cm^2/Vs$. A further increase with a considerable gradient occurs even below 50 K, and a maximum value of $165{,}000\,cm^2/Vs$ with a carrier density of $7 \times 10^{11}\,cm^{-2}$ was attained at 4 K. After illumination of the sample the mobility in the low-temperature regime is found to decrease slightly. We attribute this reduction in mobility to inter-subband scattering predicted theoretically [29]. This mechanism is expected when at higher carrier densities due to photoexcitation the first excited (also called second) subband of the quasi-triangular potential well at the heterointerface becomes occupied. In the dark as well as under illumination the observed mobility decrease for temperatures above 120 K is proportional to the relation $\mu \sim T^{-2.2}$. This value of the exponent is in good agreement with data obtained by other authors [30, 31].

The sheet carrier concentration $n_{2\,DEG}$ in selectively doped n-$Al_xGa_{1-x}As$/GaAs heterojunctions deduced from Hall effect measurements is not expected to be a function of the magnetic induction, as long as quantum oscillations of the Hall voltage do not occur, i.e. if $\mu B \ll 1$ and $B < 0.6$ T. Interpretation of the measured Hall data, however, can become more complicated if more than one conductive channel is present in the structure. A model for evaluation of data from samples having more than one conductive region, which are electrically isolated from each other, has been developed by Petriz [32] and by Larabee and Thurber [33]. If the sheet concentrations and mobilities of the two regions are n_1, n_2, and μ_1, μ_2, respectively, this model predicts for the measured Hall concentration

$$n_H = \frac{(n_1\mu_1 + n_2\mu_2)^2}{n_1\mu_1^2 + n_2\mu_2^2}. \tag{22}$$

Unfortunately, we cannot apply this model to the heterojunctions under investigation for two reasons. First, the conductive channels in selectively doped n-$Al_xGa_{1-x}As$/GaAs heterostructures are not totally isolated from one another. Secondly, Petritz [32] is using *linear* circuit theory in the model which does not allow to explain the dependence of the Hall sheet carrier concentration on the magnetic induction. In all our heterostructures with parallel conductance we observed this dependence of $n_{2\,DEG}$ vs. B, as illustrated in Fig. 9a. The increase of carrier concentration when changing the magnetic induction from 0.05 T to 0.5 T is more pronounced at 77 K than at 300 K (at 4.2 K the behaviour is similar to that at 77 K, therefore no diagram is shown). The corresponding electron mobilities of the sample vs. magnetic induction are plotted in Fig. 9b. It is important to interprete the apparent decrease of mobility with increasing B very carefully. While the sheet carrier concentration, i.e. the Hall voltage, is measured in various magnetic inductions, the conductivity of the corresponding sample is measured only at B equal to zero. The mobility is then calculated using the relation

$$\sigma^{(2)} = q n_{2\,DEG} \cdot \mu_{2\,DEG}, \tag{23}$$

where $\sigma^{(2)}$ is the 2 D conductivity. Inspection of (23) reveals that an increase of the sheet concentration $n_{2\,DEG}$ must lead to a corresponding decrease of the mobility μ, in order to keep the product $n \cdot \mu$ constant. Consequently, the apparent decrease of the mobility with B has no physical meaning and is an artefact following from (23).

The observed increase of the sheet carrier concentration with B is directly correlated with the presence

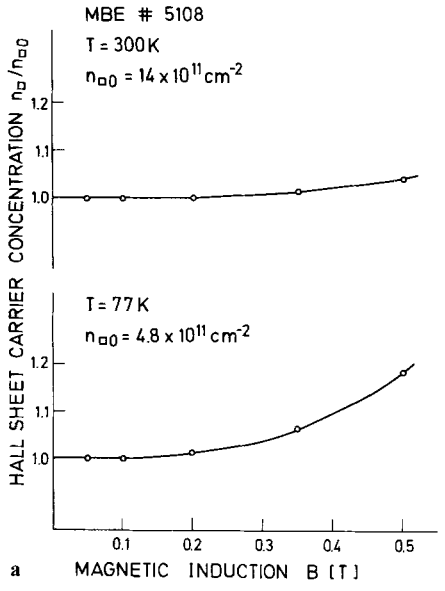

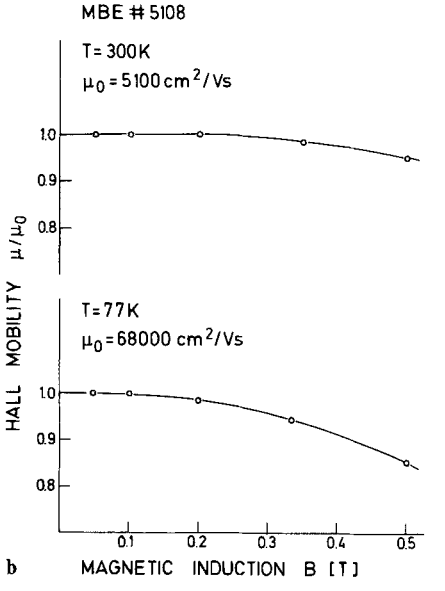

Fig. 9a and b. Hall sheet carrier concentration (a) and mobility (b) vs. magnetic induction at 300 and 77 K obtained from a selectively doped n-$Al_xGa_{1-x}As$/GaAs heterostructure with parallel conductance

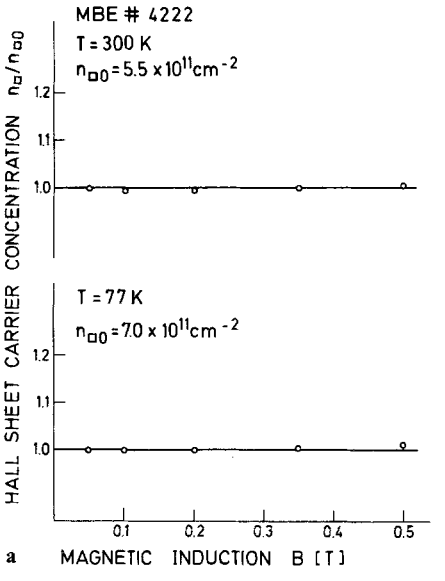

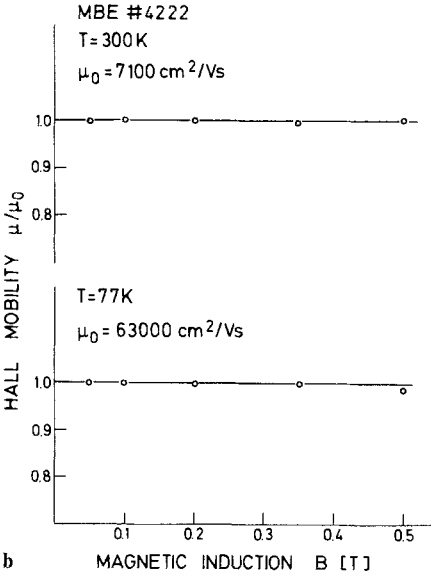

Fig. 10a and b. Hall sheet carrier concentration (a) and mobility (b) vs. magnetic induction at 300 and 77 K obtained form a selectively doped n-$Al_xGa_{1-x}As$/GaAs heterostructure with *no* parallel conductance

of an additional conductive region in the not totally depleted $Al_xGa_{1-x}As$. Therefore, also Hall measurements at different magnetic inductions can be used to detect parallel conductance in selectively doped n-$Al_xGa_{1-x}As$/GaAs heterostructures. In Fig. 10 we show the corresponding results obtained from a sample in which the 2 DEG is the only conductive channel. Neither the sheet carrier concentration nor the electron mobility vary with magnetic induction (again the behaviour at 4.2 K is similar to that at 77 K and, therefore, not shown here). This result is expected also for homogeneously doped layers.

We next try to explain the increase of Hall sheet carrier concentration with magnetic induction detected in samples with two (or more) conductive regions. For this purpose we consider the potential distribution in the sample, as indicated schematically in Fig. 11. A one-dimensional current density J is flowing through the sample, and the electric field E in the direction of the current is then

$$E = J/\sigma^{(2)} . \tag{24}$$

The electric field perpendicular to the current flow and perpendicular to the magnetic induction B in the two

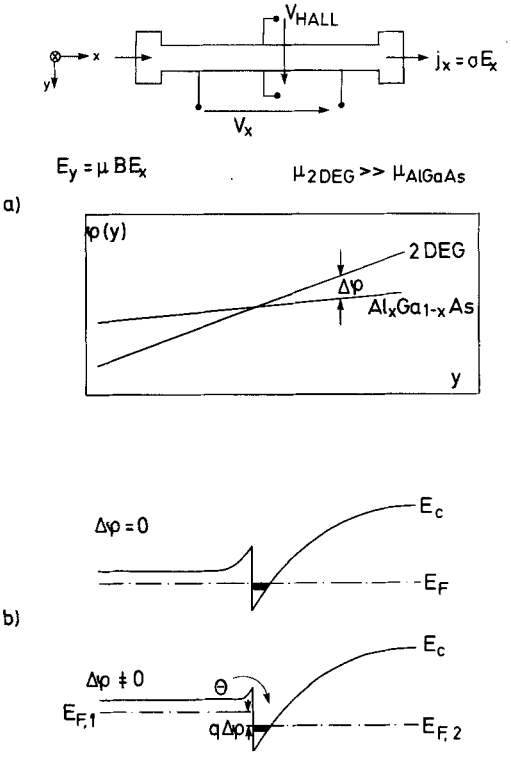

Fig. 11. (a) Schematic illustration of Hall-bar and potential distribution in a selectively doped n-$Al_xGa_{1-x}As$/GaAs heterostructure with two conductive channels. (b) Illustration of real-space transfer of electrons from the doped n-$Al_xGa_{1-x}As$ to the 2 DEG

conductive regions is given by

$$2\,\text{DEG}: \quad E_{H\,2\,\text{DEG}} = \mu_{2\,\text{DEG}} \cdot E \cdot B, \tag{25}$$

$$Al_xGa_{1-x}As: \quad E_{HP} = \mu_P \cdot E \cdot B, \tag{26}$$

where $\mu_{2\,\text{DEG}}$ and μ_P are the electron mobilities of the 2 DEG and in the not depleted $Al_xGa_{1-x}As$ layer, respectively. From the illustration in Fig. 11a we can deduce the meaning of the two different electric fields in the conductive regions. If the two conductive layers were completely isolated from each other and if no ohmic contacts were formed at the edge of the Hall-bar, two different slopes would exist for the potential. The energy band diagrams for this situation is depicted in Fig. 11b. The two differing electric Hall fields result in a splitting of the quasi-Fermi levels for the conductive regions. As electrons tend to move to lower energies, a transfer of charge in real space is expected. In the figure we have indicated that this charge transfer can only occur from the wide gap $Al_xGa_{1-x}As$ to the 2 DEG region. A reverse charge transfer is not possible because the barrier ΔE_c for electrons is *not* lowered. Consequently, an increase of the electron concentration in the 2 D accumulation channel is anticipated.

As long as the mobility of the 2 DEG is by far larger than the mobility in adjacent regions of the sample, the observed Hall electron concentration is given by the concentration of the 2 DEG. It is obvious from (25) and (26) that the quasi-Fermi level splitting becomes larger with enhanced magnetic induction. Therefore, our explanation predicts an increase of the measured Hall concentration with B. The increase should be more pronounced if the difference of the mobilities in the two conductive channels is larger. Exactly this condition is fulfilled at 77 K (and also 4 K). In homogeneously doped n-$Al_xGa_{1-x}As$:Si layers with $0.15 < x < 0.30$ we determined mobilities ranging from 1000 to 2000 $cm^2/V \cdot s$ at 77 and 300 K [28]. For the thin conductive region in the not depleted n-$Al_xGa_{1-x}As$ layer of our heterostructure we expect an even lower mobility owing to the classical size effect. The mobility of the 2 DEG, on the other hand, is found to be 6000–7000 cm^2/Vs at 300 K and 70,000–90,000 cm^2/Vs at 77 K, i.e. the mobility increases by more than a factor of ten when going to low temperatures. As a result, we observe a stronger increase of carrier concentration with magnetic induction at low temperature (see Fig. 9a) where the difference in mobility between the 2 DEG and the additional conductive channel is considerably larger.

The simple model presented here can qualitatively explain the increase of the Hall electron concentration with magnetic induction observed in selectively doped n-$Al_xGa_{1-x}As$/GaAs heterojunctions with parallel conductance. A more quantitative description requires the simulation of the behaviour by an equivalent circuit, which has not yet been developed.

3.3. Measurements of the Transverse Magnetotransport (Shubnikov-de Haas Effect)

The most sensitive method to detect even a small parallel conductance in selectively doped n-$Al_xGa_{1-x}As$/GaAs heterostructures is provided by magnetotransport measurements. The major disadvantage of this method is the requirement of a high magnetic induction ($B > 5\ T$) and of liquid He temperature to fulfill the conditions of $\mu B > 1$ and $kT < \hbar\omega_c$, where ω_c is the cyclotron angular frequency, for the occurrence of quantum oscillations of the resistance [Shubnikov-de Haas (SdH) effect].

In Fig. 12a we show the transverse magnetoresistance of a representative sample (No. 4222) at 4.2 K. With the axis of the magnetic induction normal to the plane of the 2 DEG, well defined oscillations occur in the magnetoresistance at B as low as 1 T, while no oscillations were observed when the magnetic induction was parallel to the layers. The observed oscillations, which are periodic in $1/B$, arise from variations in the

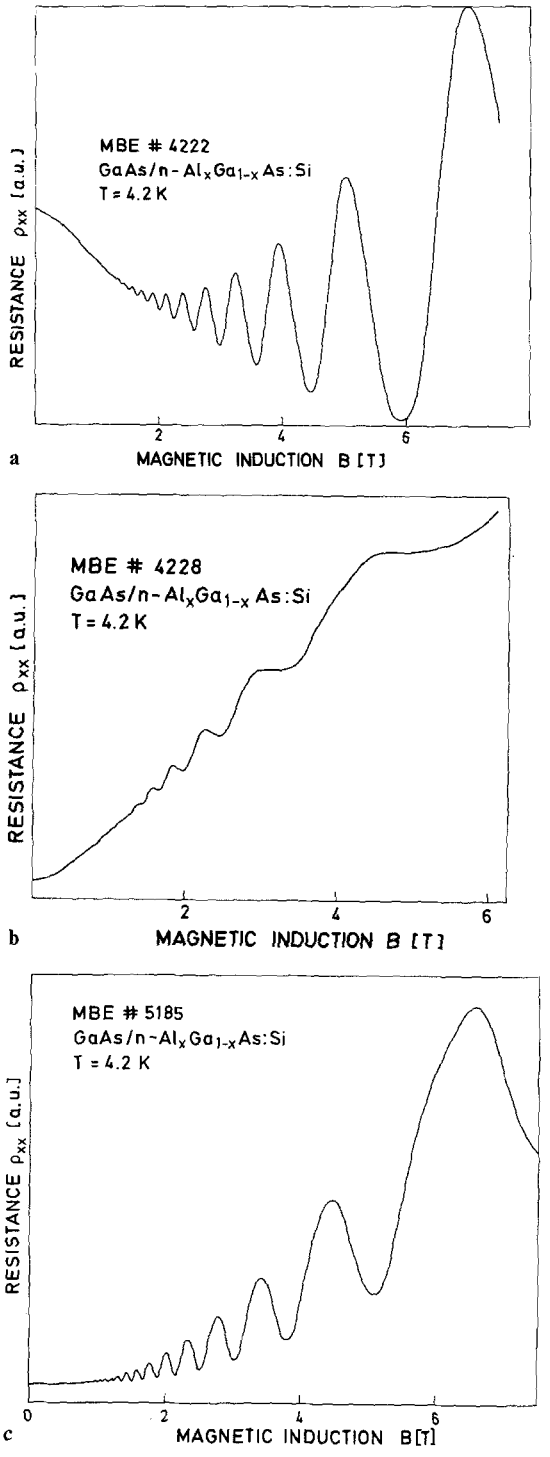

Fig. 12a–c. Transverse magnetoresistance vs. magnetic induction observed in selectively doped n-$Al_xGa_{1-x}As$/GaAs heterostructures with *no* (a), strong (b), and weak (c) parallel conductance

electron scattering behaviour as individual Landau levels cut through the Fermi energy with increasing magnetic induction (i.e. the population of the Landau levels is changed by varying B). In a two-dimensional system, the density of electrons to fill a Landau level ist $2qB/h$, where h/q is the quantum flux equal to $4.14 \times 10^{-15}\,\mathrm{Tm}^2$. From the oscillation period the electron density of the 2 DEG can be derived by using the relation

$$n_{2\,\mathrm{DEG}} = \frac{q}{\pi\hbar}\left(\Delta\frac{1}{B}\right)^{-1}. \tag{27}$$

For the specific sample under consideration we obtained $n_s = 8.8 \times 10^{11}\,\mathrm{cm}^{-2}$ which is in perfect agreement with the value of $8.8 \times 10^{11}\,\mathrm{cm}^{-2}$ deduced from 4.2 K Hall effect measurements on the same sample.

With increasing magnetic induction, the minima of the magnetoresistance oscillations become continuously lower in their ϱ_{xx} value and approach zero due to the enhanced separation of the Landau levels. From detailed investigations of the quantized Hall effect [3, 5, 6] it is now generally accepted that this typical decrease of the ϱ_{xx} minima with B clearly demonstrates the presence of only one conductive channel, i.e. the 2 DEG, in the sample. We recall that at B values where ϱ_{xx} goes to zero (fully occupied Landau levels), the value of ϱ_{xy} which is proportional to the Hall resistance becomes independent on B with values equal to $h/q^2 i$ (i = number of filled levels) [3, 4]. The explanation of the origin of the observed plateaus in ϱ_{xy} plays at present an important role in solid state physics.

In selectively doped n-$Al_xGa_{1-x}As$/GaAs heterojunctions, where the n-$Al_xGa_{1-x}As$:Si is not totally depleted, a second conductive channel for the magnetoresistance has to be taken into account. As the electron mobility in n-$Al_{0.3}Ga_{0.7}As$:Si at $T < 10\,\mathrm{K}$ is too low, a quantization in this region does not occur at the magnetic induction used in the present study. Therefore, we expect a complicated superposition of the quantum oscillations originating from the 2 DEG and of the magnetoresistance of the not depleted n-$Al_xGa_{1-x}As$:Si layer. In Fig. 12b we show the transverse magnetoresistance vs. B curve obtained from a sample (No. 4228) with a considerable parallel conductance. In this case, only a weak oscillatory behaviour is observed and the overall ϱ_{xx} values (particularly the minima) strongly increase with B which is indicative for the effect of parallel conductance. In this sample, the pronounced parallel conductance due to the not fully depleted n-$Al_xGa_{1-x}As$:Si layer is easily detected also by C-V and Hall effect measurements. The application of these other methods, however, becomes less valid for samples with only a minor parallel conductance as displayed in Fig. 12c. Here the ϱ_{xx} minima increase far less pronounced with the magnetic induction. This example illustrates that measurements of the transverse magnetoresistance at 4.2 K provide definite experimental evidence for the existence of (even a minor) second

conductive channel parallel to the 2 DEG in selectively doped n-$Al_xGa_{1-x}As$/GaAs heterojunctions. If we further determine the ϱ_{xy} values at the ϱ_{xx} minima, the expected horizontal ϱ_{xy} vs. B plateaus do not exist in samples showing parallel conductance.

Finally, we observed that the effect of parallel conductance in n-$Al_xGa_{1-x}As$/GaAs heterojunctions, where the $Al_xGa_{1-x}As$ layer is totally depleted in the dark, can be induced by illumination of the sample. The IR light emitting diode, applied as light source, prevented any band-to-band excitation in the $Al_xGa_{1-x}As$ layer. A certain time of illumination depending on illumination intensity and the properties of the individual sample was required to produce parallel conductance in the sample. The effect disappeared again when the sample was heated to room-temperature and then cooled again to 4.2 K. For measurements of the transverse magnetoresistance the light-induced parallel conductance has the same effect as its counterpart without illumination, i.e. the oscillations depicted in Fig. 12a are transferred to those of Fig. 12c.

The observed light-induced parallel conductance is caused by the fact that electrons originally bound to deep traps in the n-$Al_xGa_{1-x}As$:Si layer are photo-excited to the conduction band of the ternary alloy [14, 28]. As this excitation is persistent, the effective doping concentration $N^+_{D_{eff}}$ increases according to (16). As a consequence the depletion widths at the surface and at the heterojunction, which are inversely proportional to the doping concentration, become smaller by illumination. We have earlier pointed out (see also Fig. 2 for illustration) that parallel conductance occurs when the two depletion regions in the $Al_xGa_{1-x}As$ layers do no longer touch each other. The sheet electron concentration is then given by

$$n_p^{(2)} = N_{D_{eff}}(W - W_{DS} - W_D - W_S). \tag{28}$$

Since a dominant deep trap is known to determine the electrical properties of n-$Al_xGa_{1-x}As$ with $0.3 < x < 0.4$ [14, 28], the effective doping and thereby the depletion width of this layer in the selectively doped heterostructures can be changed significantly by illumination.

3.4. *Influence of Parallel Conductance on the Properties of Field Effect Transistors* (HEMTs)

Field effect transistors (HEMTs) of different device geometry and dimensions were fabricated from the selectively doped n-$Al_xGa_{1-x}As$/GaAs heterojunctions described in Sects. 3.1–3.3. In addition to the transistors, various other devices, including Hall-bars, Schottky contacts of different shapes and sizes for I-V and C-V measurements, and ohmic contacts for contact resistance determination, were produced on the same chip to characterize the electronic properties of the wafer. We obtained a specific ohmic contact resistance of $10^{-5}\,\Omega cm^2$ for planar Sn–Au contacts, and less than $10^{-6}\,\Omega cm^2$ for planar AuGe (eutectic)-Ni contacts, as determined with the transmission line model (TLM) [34].

For the present study, HEMTs were also made from wafers showing strong parallel conductance in addition to the 2 DEG. The effect was clearly demonstrated by additional magnetoresistance measurements on the same chip. In Fig. 13 we show that the not fully depleted $Al_xGa_{1-x}As$ layer leading to parallel conductance has a significant influence on the dc characteristics of the devices in terms of their pinch-off voltage already at 300 K operating temperature. The devices had a gate-length of 4 μm. No recessed gate was used. Examination of Fig. 13 clearly shows the drastic difference in the pinch-off voltage V_P(−1 V vs. −3 V). While the HEMT characteristic (Fig. 13a) can be described by the square law

$$\sqrt{I_{D_{sat}}} \sim V_G - V_P \tag{29}$$

according to the Shockley model, the behaviour of the transistor with parallel conductance does not follow this relation.

In addition to the pinch-off voltage, we observed a deterioration of the HEMT device characteristics by

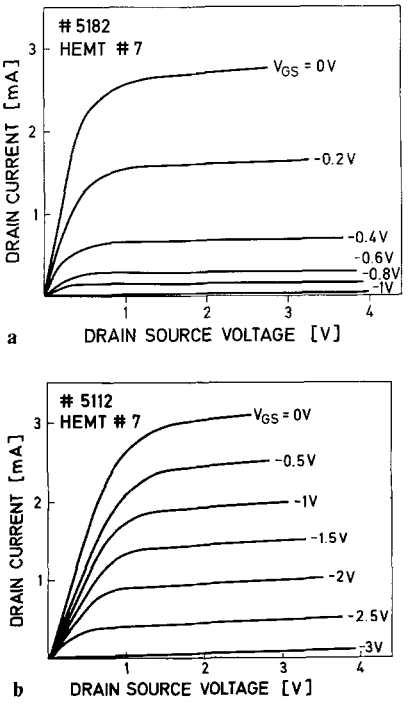

Fig. 13a and b. Typical 300 K output characteristics of a field effect transistors with 4 μm gate length fabricated from selectively doped n-$Al_xGa_{1-x}As$/GaAs heterostructures, (a) with no and (b) with strong parallel conductance

parallel conductance particularly in the high-frequency performance [10]. In the low-mobility n-$Al_xGa_{1-x}As$ layer the transit time for electrons below the gate is increased. Therefore, we expect the transit time limitation of the device to be decreased. Furthermore, the gate-to-channel capacitance C_{GS} is increased resulting in a potentially lower transit frequency according to

$$f_T = g_m/2\pi C_{GS}. \tag{30}$$

Details of the behaviour will be reported elsewhere. Besides the deteriorating effects we should emphasize, however, that the presence of parallel conductance, i.e. a not fully depleted n-$Al_xGa_{1-x}As$ layer, facilitates the formation of Ohmic contacts to the 2 DEG in selectively doped n-$Al_xGa_{1-x}As$/GaAs heterojunctions using the important AuGe-Ni metallization system.

4. Conclusion

In selectively doped n-$Al_xGa_{1-x}As$/GaAs heterostructures very high electron mobilities can be achieved particularly at low-temperatures if appropriate design parameters, i.e. alloy composition, constituent layer thickness, doping concentration etc., are chosen. If the doped $Al_xGa_{1-x}As$ region in this structure is not totally depleted from free carriers, a conductance parallel to the 2 DEG occurs which has a deleterious effect on the application of these structures in field effect transistors (HEMTs). We have shown that the occurrence of parallel conductance depends on a fairly large number of sensitive design parameters, which can in principle be calculated. However, any estimation of quantitative data required for epitaxial growth is strongly affected by the additional presence of a large amount of deep electron traps in n-$Al_xGa_{1-x}As$ of composition $0.3 < x < 0.4$, which variably reduces the final effective doping concentration. Therefore, we have employed C-V profiling, Hall effect, and transverse magnetotransport measurements to detect the undesired parallel conductance, and we have demonstrated its influence on the results of these evaluation techniques and on the properties of field effect transistors.

C-V profiling measurements on reverse-biased Schottky diodes provide the most easily accessible method to detect a pronounced parallel conductance in selectively doped n-$Al_xGa_{1-x}As$/GaAs heterostructures. While in ideal structures the depletion of the 2 DEG begins already at zero bias voltage, we observe a constant (apparent) doping concentration due to the not depleted $Al_xGa_{1-x}As$ in bypassed structures before we reach the 2 DEG at some bias voltage. Because of the differences in the dielectric constants between GaAs, $Al_xGa_{1-x}As$ and the (unknown) interfacial layer, the observed depth of the 2 DEG is always found to be larger than the actual one.

Hall effect measurements on selectively doped n-$Al_xGa_{1-x}As$/GaAs heterostructures with more than one conductive region have revealed a considerable dependence of the measured sheet carrier concentration (and thereby also of the deduced electron mobility) on the magnetic induction even in the range 0.05–0.5 T. This effect is more pronounced at low temperatures where the difference of mobilities in the two conductive channels is much larger. We have developed a simple model based on charge transfer in real space in order to interpret the observed increase of the measured Hall concentration with magnetic induction in structures with parallel conductance.

Measurements of the transverse magnetoresistance at $T < 4.2$ and $B > 5$ T with the magnetic induction normal to the plane of the 2 DEG provide the most sensitive method to detect even a minor parallel conductance. The second conductive channel implies a complicated superposition of the quantum oscillations originating from the 2 DEG and of the magnetoresistance of the not depleted n-$Al_xGa_{1-x}As$: Si layer. In this case, a less pronounced oscillatory behaviour of the magnetoresistance is observed and the minima of these oscillations do not approach zero with increasing B. This very sensitive effect can be induced also in structures without any parallel conductance in the dark by exposure of the sample to light of energy below the gap of $Al_xGa_{1-x}As$.

Finally, parallel conductance in selectively doped n-$Al_xGa_{1-x}As$/GaAs heterostructures strongly increases the pinch-off voltage of field effect transistors (HEMTs) fabricated from this material. In addition, this undesired phenomenon is expected to have an even more deleterious effect on the high-frequency performance of the device due to a decrease of the transit time limitation.

Acknowledgements. We would like to thank J. Knecht and A. Fischer for expert help in sample preparation, R. Gibis for fabricating the photolithographically defined devices, and E. Gmelin for help with the initial transverse magnetoresistance measurements. This work was sponsored by the Stiftung Volkswagenwerk.

References

1. R. Dingle, H.L. Störmer, A.C. Gossard, W. Wiegmann: Appl. Phys. Lett. **33**, 665 (1978)
2. H.L. Störmer, A. Pinczuk, A.C. Gossard, W. Wiegmann: Appl. Phys. Lett. **38**, 691 (1981)
3. K. von Klitzing, H. Obloh, G. Ebert, J. Knecht, K. Ploog: In *Precision Measurement and Fundamental Constants II*, ed. by B.N. Taylor and W.D. Phillips [Natl. Bureau of Standards (US), Spec. Publ. 617] (1981)

4. D.C. Tsui, H.L. Störmer, A.C. Gossard: Phys. Rev. B **25**, 1405 (1982)
5. D.C. Tsui, H.L. Störmer, A.C. Gossard: Phys. Rev. Lett. **48**, 1559 (1982)
6. G. Ebert, K. von Klitzing, C. Probst, K. Ploog: Solid State Commun. **44**, 95 (1982)
7. S. Hiyamizu, T. Mimura: J. Cryst. Growth **56**, 455 (1982)
8. D. Delagebeaudeuf, N.T. Linh: IEEE Trans. ED-**29**, 955 (1982)
9. K. Joshin, T. Mimura, M. Niori, Y. Yamashita, K. Kosemura, J. Saito: Microwave Theory and Technique Symposium, 1983, Technical Digest
10. H. Dämbkes, K. Heime, K. Ploog, G. Weimann: 8th European Specialist Workshop on Active Microwave Semiconductor Devices, Maidenhead, England, 1983
11. H. Künzel, H. Jung, E. Schubert, K. Ploog: J. Phys. (Paris) **43**, Colloque C5, C5–175 (1982)
12. H. Jung, A. Fischer, K. Ploog: Appl. Phys. A **33**, 97 (1984)
13. K. Hikosaka, T. Mimura, S. Hiyamizu: Inst. Phys. Conf. Ser. **63**, 233 (1982)
14. H. Künzel, K. Ploog, K. Wünstel, B.L. Zhou: J. Electron. Mater. **13** (1984) to be published
15. R. Dingle, R.A. Logan, J.R. Arthur: Inst. Phys. Conf. Ser. **33a** (1976) 210
16. G. Abstreiter, E. Bauser, A. Fischer, K. Ploog: Appl. Phys. **16**, 345 (1978)
17. H. Künzel, K. Graf, M. Hafendörfer, K. Ploog: To be published
18. S.P. Svensson, J. Kanaki, T.G. Andersson, P.O. Nilsson: Surf. Sci. **124**, L31 (1983) and references therein
C. Barrett, F. Chekir, T. Neffati, A. Vappaille, J. Massies, N.T. Linh: Physica **117** B and **118** B, 851 (1982) and references therein
19. R. Dingle: In *Advances in Solid State Physics*, ed. by H.J. Queisser (Vieweg, Braunschweig 1975) Vol. XV, p. 21
20. R.A. Smith: *Semiconductors* (Cambridge University Press, Cambridge 1978) p. 83
21. W.B. Joyce, R.W. Dixon: Appl. Phys. Lett. **31**, 354 (1977)
H. Kroemer: J. Appl. Phys. **52**, 873 (1981)
22. T. Ando, A.B. Fowler, F. Stern: Rev. Mod. Phys. **54**, 437 (1982)
23. L. Loreck, H. Dämbkes, K. Heime, K. Ploog, G. Weimann: Proc. 7th Intern. Conf. on Noise in Physical Systems, 3rd Intern. Conf. on $1/f$ Noise, Montpellier, France, Mai 1983 (to be published)
24. D.V. Lang, R.A. Logan, M. Jaros: Phys. Rev. B **19**, 1015 (1979)
25. D.P. Kennedy, P.C. Murley, W. Kleinfelder: IBM J. Res. Dev. **12**, 399 (1968)
26. K. Ploog, H. Künzel, A. Fischer: J. Electrochem. Soc. **128**, 400 (1981)
27. W.C. Johnson, P.T. Panousis: IEEE Trans. ED-**18**, 965 (1971)
28. H. Künzel, A. Fischer, J. Knecht, K. Ploog: Appl. Phys. A **32**, 69 (1983)
29. T. Ando: J. Phys. Soc. **51**, 3893 (1982)
30. S. Hiyamizu, T. Fujii, T. Mimura, K. Nanbu, J. Saito, H. Hashimoto: Jpn. J. Appl. Phys. **20**, L455 (1981)
31. T.J. Drummond, W. Kopp, R. Fischer, H. Morkoc, R.E. Thorne, A.Y. Cho: J. Appl. Phys. **53**, 1238 (1982)
32. R. Petritz: Phys. Rev. **110**, 1254 (1958)
33. R.D. Larabee, W.R. Thurber: IEEE Trans. ED-**27**, 32 (1980)
34. H.H. Berger: Solid-State Electron. **15**, 145 (1972)